Synthesis and Crystal Structure of the Iron Borate $Fe_2B_2O_5$

Stephanie C. Neumair and Hubert Huppertz

Institut für Allgemeine, Anorganische und Theoretische Chemie, Leopold-Franzens Universität Innsbruck, Innrain 52a, A-6020 Innsbruck, Austria

Reprint requests to H. Huppertz. E-mail: Hubert.Huppertz@uibk.ac.at

Z. Naturforsch. **2009**, *64b,* 491 – 498; received March 5, 2009

$Fe_2B_2O_5$, synthesized under mild high-pressure / high-temperature conditions of 3 GPa and 960 °C, possesses a structure isotypic to the triclinic pyroborates $M_2B_2O_5$ with M = Mg, Mn, Co, and Cd. Although the parameter pressure is not essential to the synthesis of $Fe_2B_2O_5$, the specific conditions enhance the crystallinity of the product. Therefore, the crystal structure of the iron pyroborate $Fe_2B_2O_5$ could be determined *via* single crystal diffraction data [space group $P\bar{1}$ (Z = 4) with the parameters a = 323.1(1), b = 615.7(2), c = 935.5(2) pm, α = 104.70(3), β = 90.82(3), γ = 91.70(3)°, V = 0.1799(1) nm^3, $R1$ = 0.0409, and $wR2$ = 0.0766 (all data)]. The structure is built up from layers of isolated pyroborate units ($[B_2O_5]^{4-}$), which are composed of two corner-sharing BO_3 triangles. These pyroborate layers serve to bridge 4×1 ribbons of edge-sharing FeO_6 octahedra by both edge- and corner-sharing.

Key words: Borate, Crystal Structure

Introduction

Crystallographic investigations of triclinic pyroborates [1 – 8] started off in the 1950ies, when S. Berger resolved the structure of $Co_2B_2O_5$ [6]. Y. Takéuchi suggested lattice parameters for the structure of $Mg_2B_2O_5$ [1], and S. Block *et al.* refined the structure of this pyroborate, classifying it as a member of the isotypic series $M_2B_2O_5$ (M = Mn, Fe, Co) [2]. Furthermore, cell parameters of $Fe_2B_2O_5$ were reported from single crystals (Buerger precession camera) by Block *et al.* [2]. However, no structural refinement of this iron borate has been reported up to now.

Under ambient-pressure conditions, five compositions are known in the ternary system Fe–B–O: $Fe^{II}{}_2Fe^{III}(BO_3)O_2$ (*Pbam*: *vonsenite* [9, 10]; $P2/m$: *hulsite* [11]), $Fe^{II}Fe^{III}{}_2(BO_4)O_2$ (*norbergite* structure) [12, 13], $Fe^{II}Fe^{III}(BO_3)O$ (*Pmcn*: *warwickite* structure [14, 15], $P2_1/c$: distorted *warwickite* structure [14, 16]), FeB_4O_7 [17, 18], and $FeBO_3$ [19]. The polymorphic phases $Fe^{II}{}_2Fe^{III}(BO_3)O_2$ and $Fe^{II}Fe^{III}(BO_3)O$, as well as the compound $FeBO_3$, consist of trigonal-planar BO_3 groups. In contrast, $Fe^{II}Fe^{III}{}_2(BO_4)O_2$ has only isolated BO_4 tetrahedra. The compound FeB_4O_7 exhibits both, BO_3 groups and BO_4 tetrahedra.

In our investigations into high-pressure / high-temperature syntheses of new iron borates, several compounds were realized, *e. g.* β-FeB_4O_7 [20] and the new polymorphs α- [21] and β-FeB_2O_4 [22]. The compounds β-FeB_4O_7 and α–FeB_2O_4 show only corner-sharing BO_4 tetrahedra, the latter being isotypic to $CaGa_2O_4$ [23], $CaAl_2O_4$-II [24, 25], and β-$SrGa_2O_4$ [26]. The compound β-FeB_2O_4 is isotypic to HP-NiB_2O_4 [27], which is the first borate having solely BO_4 tetrahedra, each sharing one common edge with a second one.

Recent research into the high-pressure / high-temperature chemistry of iron borates in our group also led to the pyroborate $Fe_2B_2O_5$. In the following, the synthesis of this compound, its crystal structure and properties are described. Furthermore, similarities and differences to the isotypic pyroborates $M_2B_2O_5$ with M = Mg [1 – 3], Mn [4, 5], Co [6, 7], and Cd [8] are discussed.

Experimental Section

According to Block *et al.*, their synthesis of $Fe_2B_2O_5$ was carried out under ambient-pressure conditions. They obtained single crystals of this compound by crystallization from the melt [2]. Although the parameter pressure is not essential to the synthesis of $Fe_2B_2O_5$, the mild high-pressure conditions used here enhanced its crystallinity. It is well known that pressure can induce amorphization or crystallization [28 – 35]. In the borates, which tend to form glasses under ambient-pressure conditions, we observed that

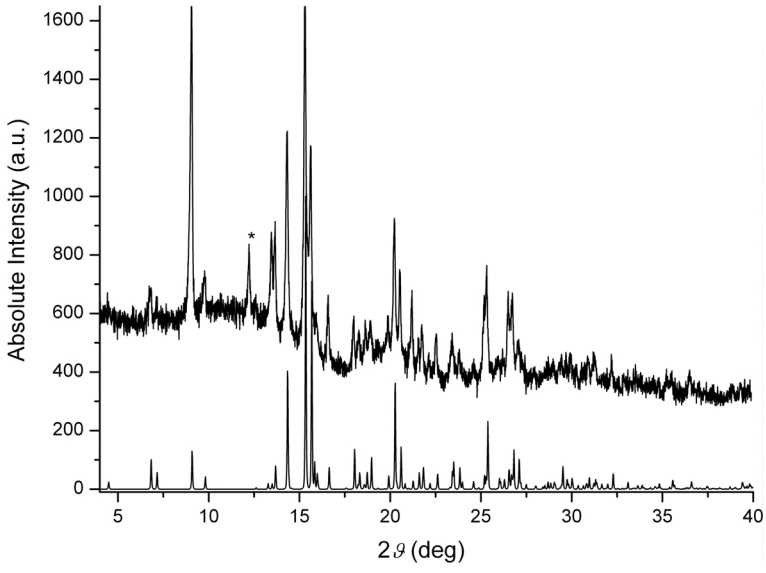

Fig. 1. Experimental powder pattern (top), compared with a theoretical powder pattern of $Fe_2B_2O_5$ (bottom); the reflection marked with an asterisk arises from hexagonal boron nitride [crucible material (JCPDS [34–421] [66])].

pressure often induces crystallization, as we could show with the examples β-SnB_4O_7 [36], β-HfB_2O_5 [37], and β-ZrB_2O_5 [38]. The pyroborate $Fe_2B_2O_5$ was also synthesized under mild high-pressure / high-temperature conditions of 3 GPa and 960 °C in a modified Walker-type multianvil apparatus. A stoichiometric mixture of Fe_2O_3 (Merck, Germany, 99 %) and B_2O_3 (Strem Chemicals, Newburyport, USA, 99.9 %) at a ratio of 1 : 1 was ground together and filled into a boron nitride crucible (Henze BNP GmbH, HeBoSint® S10, Kempten, Germany). This crucible was positioned in the center of an 18/11-assembly and compressed by eight tungsten carbide cubes (TSM-10, Ceratizit, Reutte, Austria). The pressure was applied *via* the Walker-type multianvil device and a 1000 t press (both devices from the company Voggenreiter, Mainleus, Germany). A detailed description of the assembly and its preparation is given in refs. [39 – 43]. The sample was compressed up to 3 GPa within 65 min and kept at this pressure for the heating period. The temperature was increased within 5 min to 960 °C, kept there for 10 min, and decreased to 640 °C during the next 15 min. The sample was allowed to cool down to r. t. by switching off heating, followed by a decompression period of 205 min. The recovered pressure medium was broken apart and the surrounding boron nitride crucible removed from the sample. $Fe_2B_2O_5$ was obtained as an air- and water-resistant compound in form of large moss-green crystals with acceptable quality for a single crystal structure refinement.

The reaction between Fe_2O_3 and boron oxide failed to give an Fe(III) oxoborate. Instead, the metal cation was reduced to the oxidation state 2+. A reduction of the metal ions from 3+ to lower oxidation states is often observed in the multianvil high-pressure assembly, when hexagonal boron nitride is used as crucible material [44]. Especially at elevated temperatures, pure metals are found in the reaction mixtures. A precise explanation of the redox mechanism with hexagonal boron nitride as reducing agent can not yet be given.

The elemental analysis of $Fe_2B_2O_5$ through energy dispersive X-ray spectroscopy (Jeol JFM-6500F, Jeol Ltd. Tokyo, Japan) led to values of 18 % Fe (22 %), 20 % B (22 %) and 62 % O (57 %) (theoretical values in parentheses).

Crystal structure analysis

The powder diffraction pattern of $Fe_2B_2O_5$ (Fig. 1) was obtained in transmission geometry from a flat sample of the reaction product, using a Stoe Stadi P powder diffractometer with monochromatized MoK_α (λ = 71.073 pm) radiation. The diffraction pattern was indexed with the program ITO [45] on the basis of a triclinic unit cell. The lattice parameters (Table 1) were calculated from least-squares fits of the powder data. The correct indexing of the pattern of $Fe_2B_2O_5$ was confirmed by intensity calculations, taking the atomic positions of the structure refinement [46].

For analyzing the single crystal structure, small irregularly shaped single crystals of the samples were isolated by mechanical fragmentation and examined through a Buerger precession camera, equipped with an image plate system (Fujifilm BAS-1800), to establish both, symmetry and suitability for the intensity data collection. The measurements of the single crystal intensity data were performed at r. t. by a Stoe IPDS-I diffractometer with graphite-monochromatized MoK_α (λ = 71.073 pm) radiation. All relevant details of the data collection and evaluation are listed in Table 1. To the intensity data of $Fe_2B_2O_5$, a numerical absorption correction was applied with the program

Table 1. Crystal and structure refinement data for $Fe_2B_2O_5$ (standard deviations in units of the last significant figure in parentheses).

Empirical formula	$Fe_2B_2O_5$
Molar mass, g mol^{-1}	213.32
Crystal system	triclinic
Space group	$P\bar{1}$ (no. 2)
Powder diffractometer	Stoe Stadi P
Radiation	MoK_α (λ = 71.073 pm)
Powder data	
a, pm	323.8(2)
b, pm	616.7(3)
c, pm	938.5(6)
α, deg	104.86(5)
β, deg	90.86(7)
γ, deg	91.81(5)
V, nm^3	0.1810(2)
Single crystal diffractometer	Stoe IPDS-I
Radiation	MoK_α (λ = 71.073 pm) (graphite monochromator)
Single crystal data	
a, pm	323.1(1)
b, pm	615.7(2)
c, pm	935.5(2)
α, deg	104.70(3)
β, deg	90.82(3)
γ, deg	91.70(3)
V, nm^3	0.1799(1)
Formula units per cell	Z = 2
Calculated density, g cm^{-3}	3.94
Crystal size, mm^3	0.15 × 0.11 × 0.08
Temperature, K	293(2)
Detector distance, mm	50.0
Exposure time, min	9.0
Absorption coefficient, mm^{-1}	8.0
F(000), e	204
θ range, deg	3.4 – 30.5
Range in hkl	±4, ±8, ±13
Reflections total / independent	2123 / 984
R_{int}	0.0304
Reflections with $I \geq 2\sigma(I)$	788
R_σ	0.0333
Data / ref. parameters	984 / 83
Absorption correction	numerical [47, 48]
Final $R1/wR2$ [$I \geq 2\sigma(I)$]	0.0319 / 0.0705
Final $R1/wR2$ (all data)	0.0409 / 0.0766
Goodness-of-fit on F^2	1.086
Largest diff. peak and hole, e Å^{-3}	0.85 / −0.73

X-SHAPE [47, 48]. Because of the isotypy of $Fe_2B_2O_5$ to $Co_2B_2O_5$, the atomic coordinates of $Co_2B_2O_5$ [7] were taken as starting values for $Fe_2B_2O_5$. The program SHELXL-97 [49] (full-matrix least-squares on F^2) was used for the refinement of the structure with anisotropic displacement parameters for all atoms. Final difference Fourier syntheses did not reveal any significant peaks in the refinements. Tables 2 – 5 list the positional parameters, anisotropic thermal displacement parameters, interatomic distances, and angles.

Table 2. Atomic coordinates and isotropic equivalent displacement parameters U_{eq} (Å^2) for $Fe_2B_2O_5$ (space group $P\bar{1}$ with standard deviations in parentheses. (U_{eq} is defined as one third of the trace of the orthogonalized U_{ij} tensor).

Atom	W. position	x	y	z	U_{eq}
Fe1	2i	0.7395(2)	0.20969(9)	0.36231(5)	0.0122(2)
Fe2	2i	0.2360(2)	0.36391(9)	0.10086(5)	0.0109(2)
B1	2i	0.694(2)	0.6769(7)	0.3537(4)	0.0120(7)
B2	2i	0.336(2)	0.8754(7)	0.1689(4)	0.0119(7)
O1	2i	0.2618(8)	0.6915(4)	0.0554(3)	0.0114(5)
O2	2i	0.2219(9)	0.0882(5)	0.1812(3)	0.0151(5)
O3	2i	0.7420(8)	0.4728(4)	0.2589(3)	0.0123(5)
O4	2i	0.5560(8)	0.8569(4)	0.2977(3)	0.0149(5)
O5	2i	0.7656(8)	0.7245(5)	0.4995(3)	0.0134(5)

Further details of the crystal structure investigation may be obtained from Fachinformationszentrum Karlsruhe, 76344 Eggenstein-Leopoldshafen, Germany (fax: +49-7247-808-666; e-mail: crysdata@fiz-karlsruhe.de, http://www.fiz-informationsdienste.de/en/DB/icsd/depot_anforderung.html) on quoting the deposition number CSD-420463.

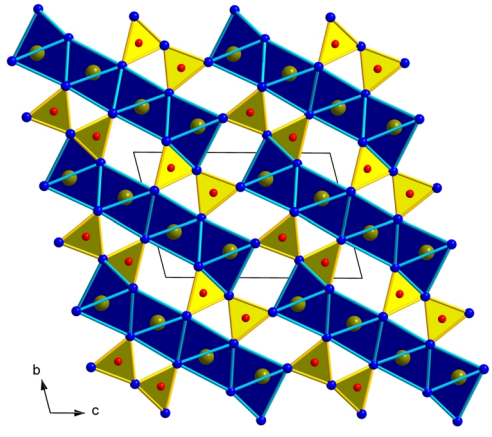

Fig. 2. (color online) Projection of the crystal structure of $Fe_2B_2O_5$, viewed along [100]. Light triangles (yellow): BO_3 groups; dark polyhedra (blue): FeO_6 octahedra.

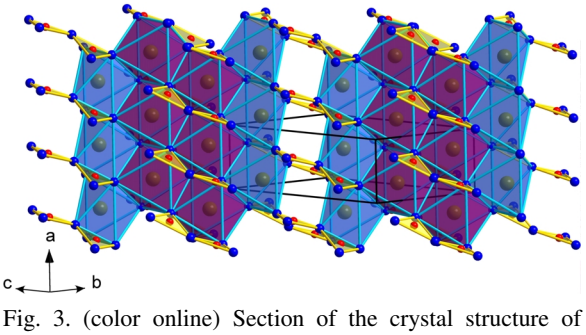

Fig. 3. (color online) Section of the crystal structure of $Fe_2B_2O_5$ with a view approximately along [011]. Light polyhedra (blue): $Fe1O_6$ octahedra; dark polyhedra (purple): $Fe2O_6$ octahedra.

Atom	U_{11}	U_{22}	U_{33}	U_{23}	U_{13}	U_{12}
Fe1	0.0127(3)	0.0112(3)	0.0125(3)	0.0028(2)	−0.0008(2)	−0.0004(2)
Fe2	0.0114(3)	0.0108(3)	0.0111(3)	0.0038(2)	−0.0006(2)	0.0009(2)
B1	0.009(2)	0.012(2)	0.016(2)	0.005(2)	0.002(2)	0.004(2)
B2	0.011(2)	0.011(2)	0.012(2)	0.002(2)	0.002(2)	−0.001(2)
O1	0.013(2)	0.009(2)	0.011(2)	0.0022(9)	−0.0004(9)	0.000(2)
O2	0.022(2)	0.010(2)	0.015(2)	0.0054(9)	0.000(2)	0.001(2)
O3	0.014(2)	0.011(2)	0.012(2)	0.0039(9)	0.0006(9)	0.003(2)
O4	0.020(2)	0.010(2)	0.015(2)	0.0032(9)	−0.004(2)	0.003(2)
O5	0.012(2)	0.017(2)	0.010(2)	0.0025(9)	−0.0008(9)	0.001(2)

Table 3. Anisotropic displacement parameters U_{ij} (Å^2) for $Fe_2B_2O_5$ (space group $P\bar{1}$) with standard deviations in parentheses.

Table 4. Interatomic distances (pm) for $Fe_2B_2O_5$ (space group $P\bar{1}$) based on single crystal data (standard deviations in parentheses).

Fe1–O5a	200.7(3)	Fe2–O2	202.3(3)	B1–O3	135.6(5)
Fe1–O5b	208.1(3)	Fe2–O1e	211.8(3)	B1–O4	142.1(4)
Fe1–O3	208.7(3)	Fe2–O3	216.1(3)	B1–O5	133.5(5)
Fe1–O4c	216.4(3)	Fe2–O1	216.4(3)		av. = 137.1
Fe1–O2	231.5(3)	Fe2–O1f	217.6(3)		
Fe1–O2d	233.0(3)	Fe2–O3g	219.3(3)	B2–O1	135.4(5)
	av. = 216.4		av. = 213.9	B2–O2h	134.9(5)
				B2–O4	142.1(4)
					av. = 137.5

Results and Discussion

As depicted in Fig. 2, the structure of $Fe_2B_2O_5$ is built up from layers of isolated $[B_2O_5]^{4-}$ units (pyroborate units), which are composed of two corner-sharing BO_3 triangles. The iron ions lie between these layers, showing a six-fold coordination by oxygen atoms. Sets of four joined FeO_6 octahedra share edges and are propagated in the direction approximately parallel to [011]. These are extended into infinite ribbons parallel to the *a* direction *via* edge-sharing. The ribbons are interconnected through pyroborate units, which have one edge- and three corner-junctions each. Thus, three adjacent ribbons are interconnected by one pyroborate anion. A view of these ribbons running along [100] is depicted in Fig. 3.

Within the pyroborate units, the BO_3 units are essentially planar, but form a dihedral angle of 16.5°.

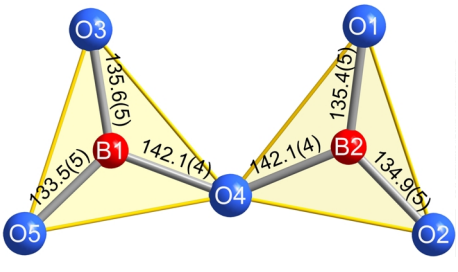

Fig. 4. (color online) Pyroborate unit in $Fe_2B_2O_5$ with bond lengths.

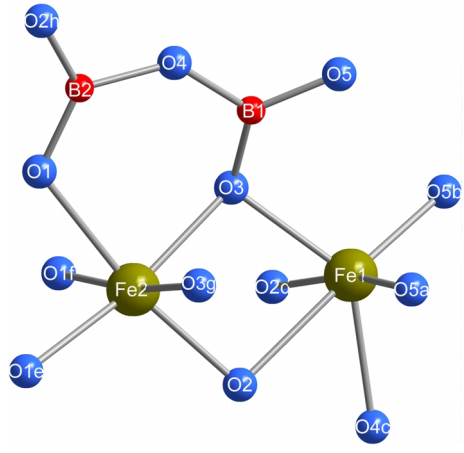

Fig. 5. (color online) Coordination scheme of boron and iron ions in $Fe_2B_2O_5$.

Both triangles are not identical, each having its different environment and bond lengths. The asymmetry of the bond lengths of the terminal and the bridging oxygen atoms are depicted in Fig. 4. The distance between boron and the bridging oxygen atom O4 is slightly increased (142.1(4) pm), compared to the terminal B–O distances, which vary between 133.5(5) and 135.6(5) pm. Notwithstanding, the average B–O bond lengths of the trigonal units are very similar (av. B1–O: 137.1, av. B2–O: 137.5 pm), corresponding to average B–O distances in BO_3 groups in other borates (av. B–O: 137.0 pm [50]). Fig. 5 shows the coordination spheres of boron and iron in $Fe_2B_2O_5$.

In the compound $Fe_2B_2O_5$, there are two crystallographically independent iron atoms, both being six-fold coordinated by oxygen atoms. The Fe–O distances in these octahedra vary in the range 200.7(3)–233.0(3) pm for Fe1, 202.3(3)–219.3(3) pm for Fe2, and average out to 215.2 pm. This average distance of 215.2 pm and the mean Fe^{2+}–O distance in other iron borates with FeO_6 octahedra (*e. g.* α-FeB_2O_4 (218.5 pm) [21] and β-FeB_2O_4 (215.3 pm) [22]) tally well.

O2–Fe1–O2d	88.14(9)	O1e–Fe2–O1	82.5(2)	O3–B1–O4	119.2(3)
O3–Fe1–O2	78.3(2)	O1–Fe2–O1f	81.5(2)	O3–B1–O5	124.8(3)
O3–Fe1–O2d	79.3(2)	O1e–Fe2–O1f	97.6(2)	O4–B1–O5	116.0(3)
O4c–Fe1–O2	61.0(2)	O2–Fe2–O1e	104.6(2)		av. = 120.0
O4c–Fe1–O2d	81.2(2)	O2–Fe2–O1f	104.4(2)		
O5b–Fe1–O2	82.5(2)	O3–Fe2–O1	89.0(2)	O1–B2–O2h	128.6(3)
O5a–Fe1–O2d	84.5(2)	O3–Fe2–O1f	82.4(2)	O1–B2–O4	120.2(3)
O5a–Fe1–O3	104.8(2)	O1–Fe2–O3g	90.1(2)	O2h–B2–O4	111.2(3)
O5b–Fe1–O3	103.1(2)	O1e–Fe2–O3g	82.95(9)		av. = 120.0
O5a–Fe1–O4c	113.0(2)	O2–Fe2–O3	83.6(2)		
O5b–Fe1–O4c	90.3(2)	O2–Fe2–O3g	83.8(2)	B1–O4–B2	135.5(3)
O5a–Fe1–O5b	104.4(2)	O3–Fe2–O3g	95.8(2)		
	av. = 89.2		av. = 89.9		

Table 5. Interatomic angles (deg) for $Fe_2B_2O_5$ (space group $P\bar{1}$) based on single crystal data (standard deviations in parentheses).

Compound	$Mg_2B_2O_5$	$Mn_2B_2O_5$	$Fe_2B_2O_5$	$Co_2B_2O_5$	$Cd_2B_2O_5$
Reactants	$Mg_2(OH)_2CO_3$, H_3BO_3	MnO, B_2O_3, $Na_2B_4O_7$	Fe_2O_3, B_2O_3	$CoCO_3$, H_3BO_3	$CdCO_3$, H_3BO_3
Temperature, °C	1200	1150	960	600 – 1100	1080
Pressure, GPa	–	–	3	–	–

Table 6. Synthetic conditions for $M_2B_2O_5$(M = Mg [1 – 3], Mn [4, 5], Fe [this work], Co [6, 7], Cd [8]).

Table 7. Comparison of the ionic radii (pm), lattice parameters (pm, deg), volumes (nm^3), and average bond lengths (pm) of $M_2B_2O_5$ (M = Mg [1 – 3], Mn [4, 5], Fe [2, this work], Co [6, 7], Cd [8]).

Compound	$r(M^{2+})$ [55, 56]	a	b	c	α	β	γ	V	av. B–O distance	av. M1–O distance	av. M2–O distance
$Mg_2B_2O_5$	86	312.1(1)	614.9(3)	922.1(8)	104.30(5)	90.29(5)	92.23(4)	0.1714(2)	137.8	209.5	210.7
$Mn_2B_2O_5$	96 (hs), 81 (ls)	327.70(1)	627.20(2)	958.80(4)	104.836(2)	90.561(2)	91.936(2)	0.18972(2)	137	222.2	220.1
$Fe_2B_2O_5$ [2]	91(hs), 75 (ls)	325(4)	618(2)	940(4)	104.10	90.37	91.29	0.1831	–	–	–
$Fe_2B_2O_5$	91(hs), 75 (ls)	323.1(1)	615.7(2)	935.5(2)	104.70(3)	90.82(3)	91.70(3)	0.17987(6)	137.3	216.4	213.9
$Co_2B_2O_5$	88 (hs), 79(ls)	316.89(3)	615.30(5)	927.34(7)	104.253(4)	90.821(4)	92.098(5)	0.17508(3)	137.6	213.2	211.3
$Cd_2B_2O_5$	109	344.90(2)	636.03(5)	995.02(8)	105.441(8)	90.807(6)	91.933(6)	0.21022(3)	137.9	239.1	233.4

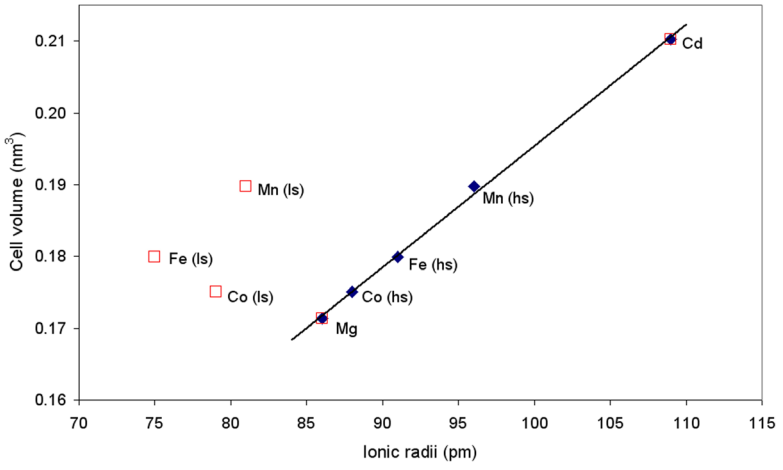

Fig. 6. Illustration of the coherence of ionic radii and cell volume of $M_2B_2O_5$ (M = Mg [1 – 3], Mn [4, 5], Fe [2, this work], Co [6, 7], Cd [8]) for the high-spin (hs, ♦) and the low-spin (ls, □) state.

The pyroborate $Fe_2B_2O_5$ presented here crystallizes isotypically to the triclinic pyroborates $M_2B_2O_5$ with M = Mg [1 – 3], Mn [4, 5], Co [6, 7], and Cd [8]. Additionally, there exist solid solutions of the composition $MM'B_2O_5$ (M = Mn, M' = Mg, Co [51], M = Zn, M' = Co, Ni [52], and M = Ca, M' = Mn [53], Mg [54]), crystallizing in the same structure type. Table 6 indicates the synthetic conditions for the isotypic ternary compounds $M_2B_2O_5$. Unfortunately, Block *et al.* did not report the starting materials for their synthesis of $Fe_2B_2O_5$ [2]. It should be noted that the mild high-pressure synthesis of $Fe_2B_2O_5$ is the only one starting from pure oxides. All other syntheses of ternary pyroborates $M_2B_2O_5$ were performed with boric acid or supported by $Na_2B_4O_7$ (flux synthesis).

Despite the isotypy, there are differences in the structures, owing to the varying ionic radii and the electronic configuration of the M^{2+} ions. Table 7 lists the different ionic radii [55,56] in both states, the high-spin (hs) and low-spin (ls) one, the lattice parameters, the mean bond lengths, and the volumes of the distinct unit cells. Fig. 6 depicts a graph of the coherence of ionic radii and cell volume. Obviously, the unit cell volume correlates only with the ionic radii for the high-spin state. Here, the compounds $M_2B_2O_5$ (M = Mn, Fe, Co) show a linear correlation to the other isotypes. In contrast, no correlation is observed for the low-spin configuration. Investigations into the magnetic susceptibility of $Mn_2B_2O_5$ revealed a magnetic moment of 5.84 μ_B [4], which reveals a high-spin configuration as well. Thus, the metal cations in $M_2B_2O_5$ (M = Mn, Fe, Co) presumably exist in the high-spin configuration. A comparison of the lattice parameters and the bond lengths reveals minor changes in a (312.1(1) – 344.90(2) pm) and b (614.9(3) – 636.03(5) pm), but remarkable variations in c (922.1(8) – 995.02(8) pm). Because the differences in the B–O distances are negligible, the reason must be found in the ionic radii of the cations. The MO_6 ribbons run along a and perpendicular to the c axis. Obviously, the change in size of the metal cations influences most strongly the size of the MO_6 octahedra along the c axis.

All triclinic pyroborates $M_2B_2O_5$ (M = Mg, Mn, Fe, Co, Cd) show two angles close to 90° in the lattice parameters. This announces a possible phase transition to the monoclinic crystal system. Up to now, a synthetic monoclinic polymorph could only be realized for $Mg_2B_2O_5$ by Guo *et al.* [57].

We calculated the bond valence sums of all atoms of $Fe_2B_2O_5$, using the bond length / bond strength (ΣV) [58, 59] and the CHARDI concept (*char*ge *di*stribution in solids, ΣQ) [60]. The results of both concepts confirm the supposed formal ionic charges, resulting from the crystal structure [ΣV: +1.98 (Fe1), +2.03 (Fe2), +3.02 (B1), +2.98 (B2), −2.00 (O1), −1.92 (O2), −2.03 (O3), −2.06 (O4), −1.97 (O5) and ΣQ: +1.99 (Fe1), +1.98 (Fe2), +2.97 (B1), +3.07 (B2), −2.05 (O1), −1.91 (O2), −2.07 (O3), −1.90 (O4), −2.07 (O5)].

Furthermore, we calculated the MAPLE values of $Fe_2B_2O_5$ (*Ma*delung *p*art of *l*attice *e*nergy) [61 – 63] to compare them with the values for the binary components, *i.e.* FeO and the high-pressure modification B_2O_3-II. This can be managed by the additive potential of the MAPLE values, which allows to calculate hypothetical values for $Fe_2B_2O_5$, starting from the binary oxides. As a result, we obtained a value of 31063 kJ/mol to be compared with 30916 kJ/mol (deviation 0.47 %), starting from the binary oxides [$2 \times$ FeO (4489 kJ mol^{-1}) [64] $+1 \times B_2O_3$−II (21938 kJ mol^{-1}) [65]].

Conclusions

High-pressure / high-temperature conditions led to high-quality crystals of the pyroborate $Fe_2B_2O_5$, which could be characterized *via* single crystal X-ray diffraction. The compound $Fe_2B_2O_5$ is isotypic to the triclinic pyroborates $M_2B_2O_5$ (M = Mg, Mn, Co, Cd) and consists of distorted FeO_6 octahedra, that form 4×1 sheets *via* edge-sharing parallel to the a axis. These sheets are interconnected through pyroborate anions ($[B_2O_5]^{4-}$), which are composed of two corner-sharing BO_3 triangles. It appears that the metal cations in $M_2B_2O_5$ (M = Mn, Fe, Co) exist in the high-spin configuration.

Acknowledgements

Special thanks go to Prof. Dr. W. Schnick, Department Chemie of the University of Munich (LMU), for the continuous support of this work. We thank T. Miller for collecting the single crystal data. This work was financially supported by the Deutsche Forschungsgemeinschaft (HU 966/2-3) and the Fonds der Chemischen Industrie.

[1] Y. Takéuchi, *Acta Crystallogr.* **1952**, *5*, 574.
[2] S. Block, G. Burley, A. Perloff, R. Mason, *J. Res. Natl. Bur. Stand.* **1959**, *62*, 95.
[3] G. Guo, W. Cheng, J. Chen, J. Huang, Q. Zhang, *Acta Crystallogr.* **1995**, *C51*, 351.
[4] J. C. Fernandes, F. S. Sarrat, R. B. Guimaraes, R. S. Freitas, M. A. Continentino, A. C. Doriguetto, Y. P. Mascarenhas, J. Ellena, E. E. Castellano, J.-L. Tholence, J. Dumas, L. Ghivelder, *Phys. Rev. B* **2003**, *67(10)*, 104413/1.
[5] F. S. Sarrat, R. B. Guimaraes, M. A. Continentino, J. C. Fernandes, A. C. Doriguetto, J. Ellena, *Phys. Rev. B* **2005**, *77(22)*, 224413/1.
[6] S. V. Berger, *Acta Chem. Scand.* **1950**, *4*, 1054.

[7] J. L. C. Rowsell, N. J. Taylor, L. F. Nazar, *J. Solid State Chem*. **2003**, *174*, 189.
[8] M. Weil, *Acta Crystallogr.* **2003**, *E59*, i95.
[9] M. Frederico, *Periodico Mineral.* **1957**, *26*,191.
[10] J. S. Swinnea, H. Steinfink, *Am. Mineral*. **1983**, *68*, 827.
[11] N. A. Yamnova, M. A. Simonov, N. V. Belov, *Kristallografiya* **1975**, *20*, 156.
[12] J. G. White, A. Miller, R. E. Nielsen, *Acta Crystallogr*. **1965**, *19*, 1060.
[13] R. Diehl, G. Brandt, *Acta Crystallogr.* **1975**, *B31*, 1662.
[14] J. P. Attfield, A. M. T. Bell, L. M. Rodriguez-Martinez, J. M. Greneche, R. Retoux, M. Leblance, R. J. Cernik, J. F. Clarke, D. A. Perkins, *J. Mater. Chem.* **1998**, *9*, 205.
[15] J. P. Attfield, A. M. T. Bell, L. M. Rodriguez-Martinez, J. M. Greneche, R. J. Cernik, D. A. Perkins, *Nature* **1998**, *369*, 655.
[16] J. P. Attfield, J. F. Clarke, D. A. Perkins, *Physica B* **1992**, *180 & 181*, 581.
[17] T. A. Kravchuk, Y. D. Lazebnik, *Russ. J. Inorg. Chem*. **1967**, *12*, 21.
[18] I. M. Rumanova, E. A. Genkina, N. V. Belov, *Latv. PSR Zinatnu Akad. Vestis Kimijas Serija* **1981**, *5*, 571.
[19] R. Diehl, *Solid State Commun.* **1975**, *17*, 743.
[20] S. C. Neumair, J. S. Knyrim, R. Glaum, H. Huppertz, *Z. Anorg. Allg. Chem.* **2009**, submitted.
[21] J. S. Knyrim, H. Huppertz, *J. Solid State Chem*. **2008**, *181*, 2092.
[22] S. C. Neumair, R. Glaum, H. Huppertz, Z. *Naturforsch*. **2009**, in preparation.
[23] H. J. Deiseroth, Hk. Müller-Buschbaum, *Z. Anorg. Allg. Chem*. **1973**, *402*, 201.
[24] S. Ito, K. Suzuki, M. Iagaki, S. Naka, *Mater. Res. Bull*. **1980**, *15*, 925.
[25] B. Lazic, V. Kahlenberg, J. Konzett, *Z. Kristallogr*. **2007**, *222*, 690.
[26] V. Kahlenberg, R. X. Fischer, C. S. J. Shaw, *J. Solid State Chem*. **2000**, *153*, 294.
[27] J. S. Knyrim, F. Roeßner, S. Jakob, D. Johrendt, I. Kinski, R. Glaum, H. Huppertz, *Angew. Chem.* **2007**, *119*, 9256; *Angew. Chem. Int. Ed.* **2007**, *46*, 9097.
[28] O. Mishima, L. D. Calvert, E. Whalley, *Nature* **1984**, *310*, 393.
[29] R. J. Hemley, A. P. Jephcoat, H. K. Mao, L. C. Ming, M. H. Manghnani, *Nature* **1988**, *334*, 52.
[30] S. K. Deb, M. Wilding, M. Somayazulu, P. F. McMillan, *Nature* **2001**, *414*, 528.
[31] C. A. Perottoni, H. A. H. Da Jornada, *Science* **1997**, *280*, 886.
[32] J. H. Nguyen, M. B. Kruger, R. Jeanloz, *Phys. Rev. Lett*. **1997**, *78*, 1936.
[33] S. M. Sharma, S. K. Sikka, *Prog. Mater. Sci*. **1996**, *40*, 1.
[34] E. G. Ponyatovsky, O. I. Barkalov, *Mater. Sci. Rep.* **1992**, *8*, 147.
[35] J. Zhang, Y. Zhao, H. Xu, M. V. Zelinskas, L. Wang, Y. Wang, T. Uchida, *Chem. Mater*. **2005**, *17*, 2817.
[36] J. S. Knyrim, F. M. Schappacher, R. Pöttgen, J. Schmedt auf der Günne, D. Johrendt, H. Huppertz, *Chem. Mater*. **2007**, *19*, 254.
[37] J. S. Knyrim, H. Huppertz, *J. Solid State Chem*. **2007**, *180*, 742.
[38] J. S. Knyrim, H. Huppertz, *Z. Naturforsch.* **2008**, *63b*, 707.
[39] N. Kawai, S. Endo, *Rev. Sci. Instrum.* **1970**, *8*, 1178.
[40] D. Walker, M. A. Carpenter, C. M. Hitch, *Am. Mineral.* **1990**, *75*, 1020.
[41] D. Walker, *Am. Mineral.* **1991**, *76*, 1092.
[42] D. C. Rubie, *Phase Transitions* **1999**, *68*, 431.
[43] H. Huppertz, *Z. Kristallogr.* **2004**, *219*, 330.
[44] J. S. Knyrim, J. Friedrichs, S. Neumair, F. Roeßner, Y. Floredo, S. Jakob, D. Johrendt, R. Glaum, H. Huppertz, *Solid State Sci*. **2008**, *10*, 168.
[45] J. W. Visser, *J. Appl. Crystallogr*. **1969**, *2*, 89.
[46] WinXPOW (version 1.2), Stoe & Cie GmbH, Darmstadt (Germany) **2001**.
[47] X-SHAPE, (version 1.05), Program for Absorption Correction, Stoe & Cie GmbH, Darmstadt (Germany) **1999**.
[48] W. Herrendorf, H. Bärnighausen, HABITUS, Program for Numerical Absorption Correction, Universities of Karlsruhe and Giessen, Karlsruhe, Giessen (Germany) **1993/1997**.
[49] G. M. Sheldrick, SHELXL-97, Program for the Refinement of Crystal Structures, University of Göttingen, Göttingen (Germany) **1997**.
[50] E. Zobetz, *Z. Kristallogr*. **1982**, *160*, 81.
[51] A. Utzolino, K. Bluhm, *Z. Naturforsch.* **1996**, *51b*, 1433.
[52] S. Busche, K. Bluhm, *Z. Naturforsch.* **1995**, *50b*, 1445.
[53] O. V. Yakubovich, M. A. Simonov, N. V. Belov, *Dokl. Akad. Nauk SSSR* **1978**, *238*, 98.
[54] O. V. Yakubovich, M. A. Simonov, N. V. Belov, *Dokl. Akad. Nauk SSSR* **1976**, *228*, 842.
[55] R. D. Shannon, C. T. Prewitt, *Acta Crystallogr.* **1969**, *B25*, 925.
[56] R. D. Shannon, *Acta Crystallogr.* **1976**, *A32*, 751.
[57] G. Guo, W. Cheng, J. Chen, J. Huang, Q. Zhang, *Acta Crystallogr.* **1995**, *C51*, 351.
[58] I. D. Brown, D. Altermatt, *Acta Crystallogr.* **1985**, *B41*, 244.
[59] N. E. Brese, M. O'Keeffe, *Acta Crystallogr.* **1991**, *B47*, 192.
[60] R. Hoppe, S. Voigt, H. Glaum, J. Kissel, H. P. Müller, K. J. Bernet, *J. Less-Common Met.* **1989**, *156*, 105.
[61] R. Hoppe, *Angew. Chem.* **1966**, *78*, 52; *Angew. Chem., Int. Ed. Engl.* **1966**, *5*, 95.

[62] R. Hoppe, *Angew. Chem.* **1970**, *82*, 7; *Angew. Chem., Int. Ed. Engl.* **1970**, *9*, 25.
[63] R. Hübenthal, MAPLE (version 4), Program for the Calculation of MAPLE Values, University of Giessen, Giessen (Germany) **1993**.
[64] H. Fjellvåg, F. Gronvøld, S. Stølen, *J. Solid State Chem.* **1996**, *124*, 52.
[65] C. T. Prewitt, R. D. Shannon, *Acta Crystallogr.* **1968**, *B24*, 869.
[66] JCPDS, International Center for Diffraction Data, Swathmore, USA, **1992**.